

Tu\_25th\_A05

## A Homotopy Optimization Method for Non-Linear Inversion of Geoelectrical Sounding Data

Z. Esmaili <sup>1\*</sup>, R. Ghanati <sup>1</sup>, M.K. Hafizi <sup>1</sup>

<sup>1</sup> University of Tehran

### Summary

---

In nonlinear inversion of geophysical data, bad initial approximation of the model parameters usually leads to local convergence of the normal Newton iteration methods, despite enforcing constraints on the physical properties. To mitigate this problem, we present a globally convergent Homotopy continuation algorithm to solve the nonlinear least squares problem through a path-tracking strategy in model space. The global convergence of the Homotopy algorithm is compared with a conventional iterative method through the synthetic and real 1-D resistivity data. Furthermore, a bootstrap-based uncertainty analysis is provided to quantify the error in the inverted models derived from the case study. The results of blocky inversion demonstrate that the proposed optimization method outperforms the Marquardt-type algorithm in the sense of the stability and the recovered models.

## 1. Introduction

Conventional iterative schemes, such as Gauss-Newton's method, Landweber iterative scheme, and the conjugate gradient algorithm may converge to various local minima if the starting model is far from the convergence region of a global minimum of the cost function so that slight variations in starting point can lead to a significantly different Earth model. A remedy to the exiting problem is to use derivative-free global direct search techniques (e.g., Monte Carlo, simulated annealing, and genetic algorithm), which are less dependent on initial model compared to local search approaches. However, it should be noted that the computational cost of the global optimization approaches strongly depends on the size of the parameter space. In this paper, we present and develop an alternative approach based upon Homotopy continuation optimization method attempting to overwhelm the above limitations. Homotopy is a powerful tool for solving a vast range of nonlinear problems due to its widely convergent properties for almost all choices of the initial model (Watson and Haftka, 1989; Axelsson and Sysala, 2015; Yu, et al, 2016). Despite successful applications of the Homotopy algorithm to nonlinear inverse problems in the mathematical literature, there are still few applications in the context of geophysics.

The general objective of this study is to show an efficient implementation of the Homotopy continuation method to regularization vertical electrical sounding. The presented algorithm is tested and compared with a Marquardt-type inversion using a synthetic and a real data set.

## 2. Methodology

The method is based on the idea of solving a sequence of nonlinear problems that vary gradually from an arbitrary initial problem, having at least one known solution, to the final problem to be solved, using each step's solution as the next step's starting model.

### 2.1. A General Homotopy

Considering the following system of nonlinear equations

$$\mathbf{F}(\mathbf{m}) = 0 \quad (1)$$

Where  $F: \mathbb{R}^n \rightarrow \mathbb{R}^n$  and without a suitable starting point, an iterative solution to Equation (1) may converge to a local minimum of the penalty function rather than to a solution of the nonlinear system. To resolve the problem, instead of looking into the original problem  $\mathbf{F}(\mathbf{m}) = 0$  directly, a parameter depending function, known as Homotopy continuation function,  $\mathcal{H}$  in variables  $\mathbf{m}$  and  $\mathfrak{S}$ , is generally defined (Watson and Haftka, 1989)

$$\mathcal{H}(\mathbf{m}, \mathfrak{S}) = \zeta(\mathfrak{S})\mathbf{F}(\mathbf{m}) + \chi(\mathfrak{S})\mathbf{P}(\mathbf{m}) \quad (2)$$

Where  $\mathcal{H}: \mathbb{R}^n \times \mathbb{R} \rightarrow \mathbb{R}^n$ ,  $\mathbf{F}(\mathbf{m})$  indicates original problem (or target function),  $\mathbf{P}(\mathbf{m})$  is auxiliary continuation function with obtainable unique solution  $\mathbf{m}_0$ , and  $\mathfrak{S} \in [0,1]$  is continuation parameter such that  $\zeta(0) = \chi(1) = 0$ ,  $\zeta(1) = \chi(0) = 1$  and  $\zeta(\mathfrak{S}) > 0$ ,  $\chi(\mathfrak{S}) > 0$  whenever  $0 < \mathfrak{S} < 1$ .

Equation (2) simplifies to

$$\mathcal{H}(\mathbf{m}, \mathfrak{S}) = \mathfrak{S}\mathbf{F}(\mathbf{m}) + (1 - \mathfrak{S})\mathbf{P}(\mathbf{m}) \quad (3)$$

by replacing  $\zeta(\mathfrak{S})$  and  $\chi(\mathfrak{S})$  with  $\mathfrak{S}$  and  $(1 - \mathfrak{S})$ , respectively. The convex function  $\mathcal{H}$  provides us with a continuous deformation from the auxiliary function for  $\mathfrak{S} = 0$  through  $\mathcal{H}(\mathbf{m}, 0)$  to the target function for  $\mathfrak{S} = 1$  through  $\mathcal{H}(\mathbf{m}, 1)$ . The implementation of the algorithm is carried out by monotonically increasing the continuation parameter  $\mathfrak{S}$  from zero to unit and calculating the solution of the system

$\mathcal{H}(\mathbf{m}, \mathfrak{S}) = 0$  for each value of  $\mathfrak{S}$ . The final value of  $\mathfrak{S} = 1$  will be a solution for the target function  $F(\mathbf{m}) = 0$ .

## 2.2. Extension of Homotopy to Nonlinear Least-Squares Problem

The minimal least squares can be formulated as the following unconstrained problem

$$\min_{\mathbf{m} \in \mathbb{R}^n} \psi(\mathbf{m}) := \|\mathcal{W}_\eta(G(\mathbf{m}) - \mathbf{y}_\delta)\|_{\ell_2}^2 \quad (4)$$

Where  $G \in \mathbb{R}^{m \times n}$  is the nonlinear forward operator mapping the model parameters  $\mathbf{m} \in \mathbb{R}^{n \times 1}$  to the noisy data  $\mathbf{y}_\delta \in \mathbb{R}^{m \times 1}$  spaces, and  $\mathcal{W}_\eta$  displays the data weighting matrix.

The obtained solution of the minimization of  $\psi(\mathbf{m})$  will be unstable and physically unrealistic due to the ill-posedness of the forward operator matrix. Hence, regularization strategies, which have become an integral portion of the inverse problem theory, need to be enforced on the inversion problem to overcome the instabilities and solve the problem. Thus, a regularized Gauss-Newton method combined with a Homotopy continuation method is used. The regularized Homotopy strategy either alleviates the numerical effects of the illposedness or append global convergence properties to the inversion algorithm. In the context of least squares problem, a Homotopy continuation function is constructed by replacing  $F(\mathbf{m})$  and  $P(\mathbf{m})$  in Equation (3) with  $\mathbf{y}_\delta$  and  $G(\mathbf{m}_0)$ , respectively, so that

$$\mathcal{H}(\mathbf{m}, \mathfrak{S}) = \mathfrak{S}\mathbf{y}_\delta + (1 - \mathfrak{S})G(\mathbf{m}_0). \quad (5)$$

where  $G(\mathbf{m}_0)$  is the forward response of the problem in terms of the starting model  $\mathbf{m}_0$ . The interval  $[\mathfrak{S} = 0, \mathfrak{S} = 1]$  is equally divided into  $N$  continuation parameters. Then an iteratively regularized Gauss-Newton is applied to minimize the objective function at the  $q$ th step of the Homotopy continuation Eq. (5). The iterative numerical method is thus given as follows:

$$\begin{aligned} \Delta \mathbf{m}_q^\ell &= \alpha_q \left( \mathbf{J}^T(\mathbf{m}_{q-1}) \mathcal{W}_\eta^T \mathcal{W}_\eta \mathbf{J}(\mathbf{m}_{q-1}) + \beta^\ell \mathcal{W}_m^T \mathcal{W}_m \right)^{-1} \\ &\times \left[ \mathbf{J}^T(\mathbf{m}_{q-1}) \mathcal{W}_\eta^T \mathcal{W}_\eta \left( G(\mathbf{m}_{q-1}) - \mathcal{H}(\mathbf{m}, \mathfrak{S}_\ell) \right) - \beta^\ell \mathcal{W}_m^T \mathcal{W}_m (\mathbf{m}_{q-1} - \mathbf{m}_{apr}^\ell) \right], \end{aligned} \quad (6)$$

where  $\ell$  and  $q$  implies the iteration indices of the Homotopy steps and the regularized Gauss-Newton iterations, respectively,  $\alpha_q$  is the step length with positive value which controls the rate of convergence,  $\mathbf{J}$  is the Jacobian operator,  $\mathcal{W}_m$  is the model weighting matrix,  $\mathbf{m}_{apr}$  allows specification of a given reference vector of prior information for the model parameters  $\mathbf{m}$ .

Substituting Eq. (5) into Eq. (6), the update  $\Delta \mathbf{m}$  to the mode  $\mathbf{m}$  is recovered by solving

$$\begin{aligned} \Delta \mathbf{m}_q^\ell &= \varepsilon_q \left( \mathbf{J}^T(\mathbf{m}_{q-1}) \mathcal{W}_\eta^T \mathcal{W}_\eta \mathbf{J}(\mathbf{m}_q) + \beta^\ell \mathcal{W}_m^T \mathcal{W}_m \right)^{-1} \\ &\times \left[ \mathbf{J}^T(\mathbf{m}_{q-1}) \mathcal{W}_\eta^T \mathcal{W}_\eta \left( (\mathfrak{S}_\ell \mathbf{y}_\delta + (1 - \mathfrak{S}_\ell)G(\mathbf{m}_0)) - G(\mathbf{m}_{q-1}) \right) - \beta^\ell \mathcal{W}_m^T \mathcal{W}_m (\mathbf{m}_{q-1} - \mathbf{m}_{apr}^\ell) \right]. \end{aligned} \quad (7)$$

Furthermore, to avoid physically unrealistic model parameter estimates, lower and upper bounding constraints are imposed. Constraints restrict variations in the model parameters during the inversion process such that unreasonable solutions are alleviated.

## 3. Numerical Examples

### 3.1. Synthetic data

A synthetic earth model consisting of unsaturated layer, a freshwater aquifer, a clay layer, and a saltwater aquifer beneath. To create the synthetic data, a schlumberger configuration with 25 AB/2 spreads ranging from 1.25 to 1000 m is conducted on the simulated earth model with the assumed

parameters represented in Table 1. Then the forward modeling responses are perturbed by a 3 % of Gaussian noise. Figure 1 shows the subsurface resistivity models obtained from inverting the synthetic data using the proposed method (left panel) and a Marquardt-type algorithm (right panel). In addition, a statistical analysis based on 10 different noise realizations are reported in Table 1. From Table 1, it is clear that the proposed method converges and recovers the true parameters accurately while the Levenberg-Marquardt procedure provided only a rough approximation of the true parameters.

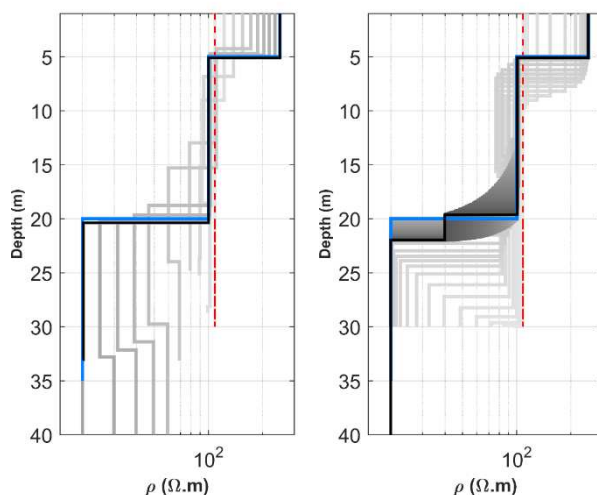


**Figure 1.** Inversion result of the synthetic model with the first starting model using the Homotopy continuation procedure (left panel) compared with a Marquardt-type inversion result (right panel). Color variation from gray to black indicates increasing number of iterations.

**Table 1.** Numerical results of the synthetic modeling using the proposed algorithm and a Marquardt-type method. The starting model includes a four-layered earth with the mean of the apparent resistivity values and thicknesses of 10 m.

Layer	True model	Inverted parameters via Homotopy-based method	Inverted parameter Levenberg-Marquardt-based method
1	$\rho_1 = 250$ $h_1 = 5$	$\rho_1 = 250.03(0.25)$ $h_1 = 4.98(0.15)$	$\rho_1 = 249.89(0.26)$ $h_1 = 5.05(0.1)$
2	$\rho_2 = 100$ $h_2 = 15$	$\rho_2 = 100.34(1.4)$ $h_2 = 14.93(0.45)$	$\rho_2 = 99.75(2.98)$ $h_2 = 8.94(3.83)$
3	$\rho_3 = 20$ $h_3 = 15$	$\rho_3 = 20.09(0.14)$ $h_3 = 17.85(5.12)$	$\rho_3 = 79.78(26.27)$ $h_3 = 7.02(3.04)$
4	$\rho_4 = 20$	$\rho_4 = 19.98(0.05)$	$\rho_4 = 20.02(0.5)$

### 3.2. Real data

We eventually provide a field data set with a known geology information for field-scale verification. The DC resistivity sounding data measurement has been conducted through the Schlumberger array consisting of 23 apparent resistivity records with current electrode spacing ranging from 3 to 47 m. This site was chosen on the basis of the accessibility of a nearby lithology borehole information. Based on the drill hole, the geology section is characterized by a vadose zone with a thickness of 3 m, followed by a fresh water-bearing layer composed of fine sand and clayey sand until a depth of 10 m, underlined by a 9 m mudstone followed by mudstone mixed with siltstone layer until the bottom of the borehole. Figure 2 shows the subsurface resistivity models obtained from inverting the field data using the

proposed method (left panel) and a Marquardt-type algorithm (right panel). Comparing the resulting models, it is evident that there is a much better agreement between the geo-electrical parameters inverted using the proposed method and the ground truth. Figure 2 also represents equivalent models from the bootstrap uncertainty analysis (gray line). Looking at the bootstrap uncertainty, it can be seen that the resistivity and thickness values retrieved using the proposed approach have smaller uncertainties compared to those of the Levenberg-Marquardt method.

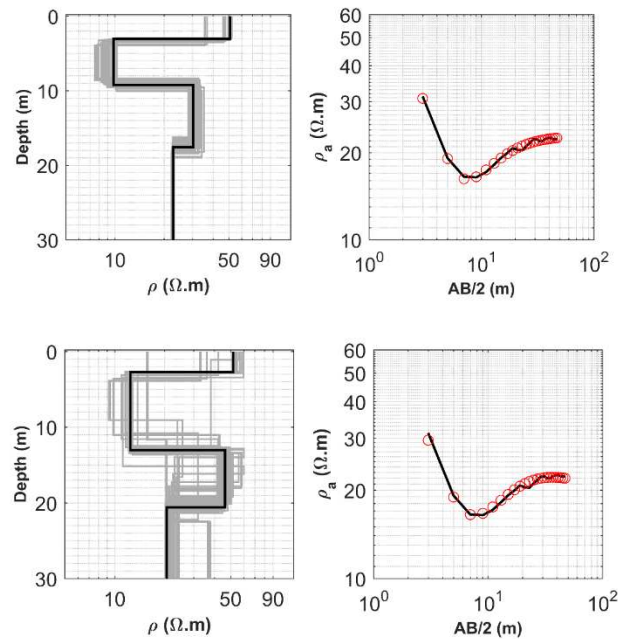


**Figure 2.** Inversion results of the case study, Left column: Inverted models (black curve) via the Homotopy algorithm (top panel), and the Marquardt-Levenberg method (bottom panel) accompanying with bootstrap uncertainty analysis (grey curve). Right column: measured data (black curve) and fitted model response (red circle) corresponding to the Homotopy inversion (top panel) and the Marquardt-Levenberg method (bottom panel).

#### 4. Conclusions

We have presented a novel application of the Homotopy continuation inversion, to geo-electrical sounding inverse problems. We applied the method to invert two synthetic examples and a real data set in the case of 1D blocky models. Comparing with the inversion results by a Marquardt-type method, the proposed algorithm can create more stable and accurate estimations and converge toward satisfactory results at a faster rate.

#### 5. References

- Axelsson, O., Sysala, S., 2015. Continuation Newton methods, *Computers and Mathematics with Applications*, 70, 2621–2637.
- Watson, L.T., Haftka, R.T., 1989. Modern homotopy methods in optimization, *Comput. Methods Appl. Mech. Eng.*, 74,289–305.
- Yu, C.X., Zhao, J.T., Wang, Y.F., Qiu, Z., 2016. Sparse diffraction imaging method using an adaptive reweighting homotopy algorithm, *J. Geophys. Eng.*, 14, 26.